Polymer 54 (2013) 5214–5221

Contents lists available at ScienceDirect

Polymer

journal homepage: www.elsevier.com/locate/polymer

Insights into the coordination sphere of copper ion in polymers containing carboxylic acid and azole groups

Juan M. Lázaro-Martínez [a,b], Gustavo A. Monti [a], Ana K. Chattah [a,*]

[a] FaMAF-Universidad Nacional de Córdoba & IFEG-CONICET, Medina Allende s/n, X5000HUA Córdoba, Argentina
[b] Departamento de Química Orgánica, Facultad de Farmacia y Bioquímica, Universidad de Buenos Aires, Junín 956, C1113AAD Ciudad Autónoma de Buenos Aires, Argentina

ARTICLE INFO

Article history:
Received 10 May 2013
Received in revised form
11 July 2013
Accepted 15 July 2013
Available online 23 July 2013

Keywords:
Copper complexes
Solid-state NMR
EPR

ABSTRACT

In this work, we describe the Cu^{2+} ion uptake from recently developed hydrogel with polyampholyte and polyelectrolyte behavior at different concentrations of the metal ion. Solid-state NMR and EPR were used as complementary techniques to understand the coordination role of carboxylic acid and azole groups (imidazole, triazole and pyrazole) involved in the copper ion coordination. In polymers containing imidazole and triazole, the uptake took place preferentially through the azole groups, with less participation of the carboxylate groups at low concentrations of Cu^{2+}. However, as the concentration of Cu^{2+} increased, these azole ligands became less active in the new sites for copper. In polymers containing pyrazole, coordination of Cu^{2+} was through both carboxylate and pyrazole ligands, regardless of the concentration of Cu^{2+}.

Interactions of the different ligands in the networks and the structural changes produced by copper ions (Cu^{1+}, Cu^{2+}) were characterized by thermal and NMR measurements.

1. Introduction

Macromolecular chemistry has become of great interest to yield processable materials with unique and valuable properties. Among them, polymer networks offer new possibilities to scientists for the creation of artificial materials [1–3]. In particular, incorporating coordination complexes into polymeric architectures opens up the possibility of imparting the physicochemical properties of both partners to the resulting material [4–6]. In recent years, hydrogels with chelating ligands have attracted attention for industrial applications, such as the removal of toxic heavy metal ions from aqueous media [7–12] and the recovery of gold from HCl solutions [13]. Metallo-hydrogels [14–19] have also been used for biomedical applications such as the controlled delivery of proteins [20], probes, sensors, imaging agents, macromolecular catalysts, artificial enzymes, and stimuli-responsive materials [21]. Adsorbents for the removal of copper ion from aqueous solution are particularly useful due to the catalytic activity of the resulting Cu(II)-polymer complex. These complexes have been used as heterogeneous catalysts for H_2O_2 activation with the concomitant degradation of organic pollutants [22–25], showing better performance than the homogenous catalysts. Furthermore, some Cu(I)- or Cu(II)-polymer complexes have demonstrated biomimetic activities [26,27] and Challa et al. analyzed the effect of Cu(II) coordination sphere in the catalytic performance of immobilized Cu(II)-complexes of imidazole-containing polymers for the oxidative coupling of 2,6-disubstituted phenols [28,29]. In particular, copper-imidazole systems have been used as models to understand the biological activity of proteins involved in Alzheimer's disease and prion infection [30–33].

We have previously demonstrated that solid-state NMR is a powerful technique to characterize hydrogels and their Cu(II)-complexes. Particularly, we have observed that the carbon signal of the carboxylic acid in the ^{13}C CP-MAS spectra (cross-polarization and magic angle spinning) is a sensitive parameter to sense the union of Cu(II) to this ligand (RCO_2H) [34]. Chen et al. have also observed similar changes in the ^{13}C NMR spectra in solution for Sm(III)-hyperbranched *poly*(ester-amide) [35].

In this work, we describe the Cu^{2+} ion uptake from different hydrogels with polyampholyte and polyelectrolyte behavior at different concentrations of the metal ion. Solid-state NMR and EPR techniques were used to understand the coordination role of carboxylic acid and heterocyclic azole groups (imidazole, triazole and pyrazole) involved in the copper ion coordination sphere. Changes

* Corresponding author. Tel./fax: +54 351 4334051.
E-mail addresses: chattah@famaf.unc.edu.ar, kchattah@gmail.com (A.K. Chattah).

0032-3861/$ – see front matter © 2013 Elsevier Ltd. All rights reserved.
http://dx.doi.org/10.1016/j.polymer.2013.07.036

in the structural network were observed by a combination of thermal characterization (TG/DTG) and NMR experiments performed in the loaded and unloaded polymers.

2. Experimental

2.1. Materials and methods

Polymer materials were synthesized with ethylene glycol diglycidyl ether (EGDE), methacrylic acid (MAA) and/or nitrogen-heterocycle monomers (IM = imidazole, 2MI = 2-methylimidazole, PYR = pyrazole, or TRZ = triazole) as described previously [36]. The representative chemical structure for the different polymers and their corresponding abbreviation names used throughout the manuscript are show in Figs. 1–4. The degree of disubstitution of the azole units (Het^+) in the different materials was determined by substraction of the protonated groups ($HetH^+$), determined from titration with a NaOH standard solution, to the total of protonable and disubstituted azole units (Het^+OH^-), determined from titration with a HCl standard solution [36].

The different Cu(II) complexes were obtained from the adsorption of Cu^{2+} ions on the different polymers by batch adsorption experiments. Each material (0.1000 g) was placed in contact with 2 mL of cupric sulfate ($CuSO_4$) solution in a 4–100 mM concentration range. The resulting suspensions were shaken in a thermostatic bath at 25 °C for 24 h. Then, the samples were centrifuged, filtered and the free copper ion concentration in each supernatant solution was determined spectrophotometrically since $[Cu(NH_3)_4]^{2+}$, formed by ammonium hydroxide addition, absorbs radiation at 640 nm. All the experiments were performed in duplicate. The adsorption data were fitted according to the linear Langmuir model:

$$\frac{C_e}{q_e} = \frac{C_e}{q_m} + \frac{1}{K_L \times q_m} \quad (1)$$

where q_m is the maximal adsorption capacity of the copper ion on the different adsorbents (mg g^{-1}) and K_L is the adsorption equilibrium constant (L mg^{-1}). The Freundlich model was also explored but it was not used because the correlation coefficients (R^2) were lower (<0.899) than the values obtained with the Langmuir model

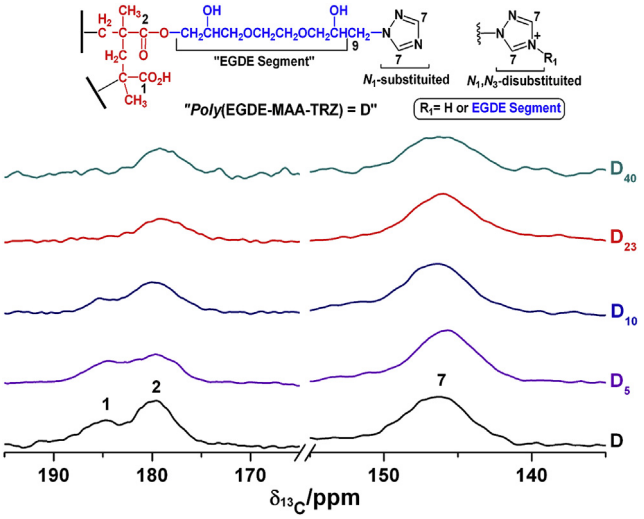

Fig. 1. High frequency regions of the ^{13}C CP-MAS spectra for polymer D, D_5, D_{10}, D_{23} with a contact time of 1.5 ms and D_{40} with a contact time of 800 μs. In all the samples, the number of scans was 2000.

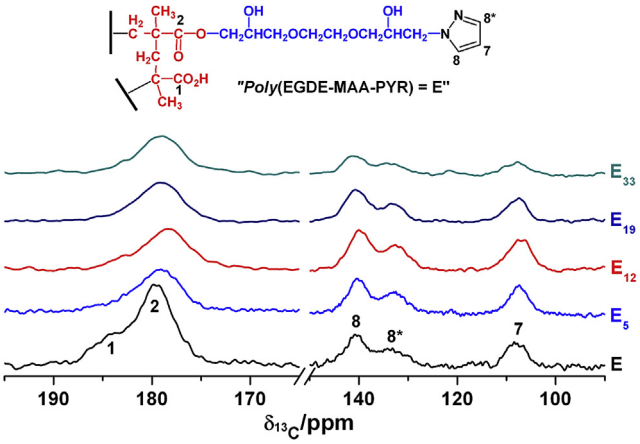

Fig. 2. High frequency regions of the ^{13}C CP-MAS spectra for polymer E, E_5, E_{12} and E_{19} with a contact time of 1.5 ms and E_{33} with a contact time of 800 μs. In all the samples, the number of scans was 2000.

(>0.999). The resulting Cu(II)-complexes were washed with deionized water and dried at 60 °C for 24 h.

The following abbreviations are used throughout the manuscript:

- A: Poly(EGDE-MAA).
- A_1: Cu(II)-Poly(EGDE-MAA) with 1 mg of Cu(II) per gram of polymer.
- B: Poly(EGDE-MAA-IM).
- B_x: Cu(II)-Poly(EGDE-MAA-IM) with x mg of Cu(II) per gram of polymer.
- C: Poly(EGDE-2MI).
- C_x: Cu(II)-Poly(EGDE-2MI) with x mg of Cu(II) per gram of polymer.
- D: Poly(EGDE-MAA-TRZ).
- D_x: Cu(II)-Poly(EGDE-MAA-TRZ) with x mg of Cu(II) per gram of polymer.
- E: Poly(EGDE-MAA-PYR).
- E_x: Cu(II)-Poly(EGDE-MAA-PYR) with x mg of Cu(II) per gram of polymer.

The Cu(I,II)-complex B_{63}^{T1} was obtained from B_{63} when it was treated as a heterogeneous catalyst for H_2O_2 activation in 0.1 M phosphate buffer at pH 7.0. A 100.0 mL aliquot of a solution

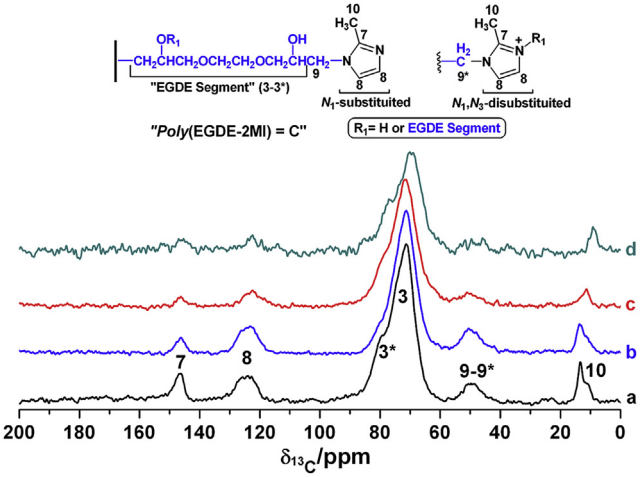

Fig. 3. ^{13}CP-MAS spectra for polymer C with contact times of 1500 (a) and 600 μs (b) and for the Cu(II)-complexes C_{60} with different contact times: 600 (c) and 1000 μs (d). In all the samples, the number of scans was 2000.

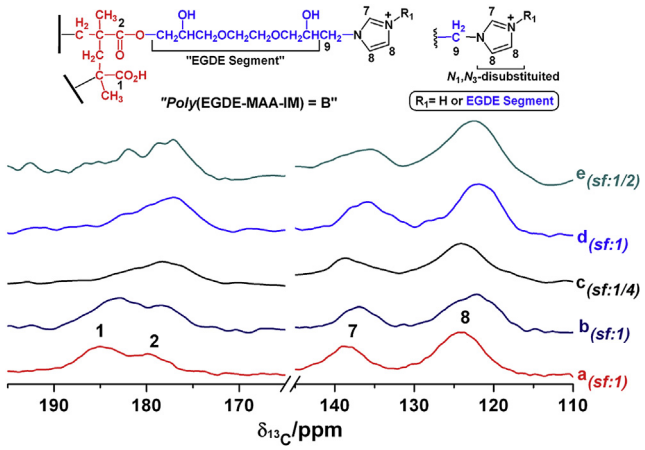

Fig. 4. High frequency regions of the ^{13}C CP-MAS spectra for polymer B (a) and B^{T2} (b) with a contact time of 1.5 ms, B_{63} (c), B_{63}^{T1} (d) and B_{63}^{T2} with 800 μs of contact time (e). (*sf*: scaling factor). In all the samples, the number of scans was 2000.

containing H_2O_2 was put in contact with 500.0 mg of the catalyst B_{63}. The initial concentration of H_2O_2 was 50 mM. After 3 h of reaction, the catalyst was separated from the solution, washed with deionized water and dried at room temperature.

The B^{T2} material was prepared from the treatment of polymer B with a 1 M NaOH solution for 24 h. Then, B^{T2} was separated from the alkaline solution, washed with deionized water and dried at 60 °C for 24 h.

The Cu(II)-complex B_{63}^{T2} was obtained from the adsorption of Cu^{2+} ions on the B^{T2} material as described previously in this section.

All the copper complexes were properly dried and placed in a desiccator for further NMR, EPR and thermal studies.

In particular, the surface of B and B_{63} was characterized using a scanning electron microscope Field Emission SEM (Zeiss Gemini DSM 982) operated at a 0.3 kV acceleration voltage.

2.2. Solid-state nuclear magnetic resonance (ssNMR)

High-resolution ^{13}C solid-state spectra for the polymers were recorded using the ramp $\{^1H\} \rightarrow \{^{13}C\}$ CP-MAS pulse sequence (cross-polarization and magic angle spinning) with proton decoupling during acquisition. All the solid-state NMR experiments were performed at room temperature in a Bruker Avance II-300 spectrometer equipped with a 4-mm MAS probe. The operating frequency for protons and carbons was 300.13 and 75.46 MHz, respectively. Glycine was used as an external reference for the ^{13}C spectra and to set the Hartmann-Hahn matching condition in the cross-polarization experiments. The recycling time was 4 s. Different contact times during CP were employed in the range of 500–1500 μs. The SPINAL64 sequence (small phase incremental alternation with 64 steps) was used for heteronuclear decoupling during acquisition with a proton field H_{1H} satisfying $\omega_{1H}/2\pi = \gamma_H H_{1H} = 62$ kHz [37]. The spinning rate for all the samples was 10 kHz.

The proton and carbon NMR spin-lattice relaxation times in the rotating frame ($T_{1\rho}^H$ and $T_{1\rho}^C$) were measured via CP-MAS carbon spectra for the polymers and their copper-complexes. To measure $T_{1\rho}^H$ and $T_{1\rho}^C$, proton and carbon spin-lock fields at $\omega_{1H}/2\pi = 40$ kHz and $\omega_{1C}/2\pi = 53$ kHz were inserted as a function of a variable time τ, before and after the contact time step, respectively. The time τ was varied from 10 μs to 6 ms. The contact time was 100 μs, short enough to avoid spin diffusion between protons. The spinning rate for all the samples was 10 kHz.

The 2D ^1H-^{13}C wideline separation experiment (2D WISE) was performed following the pulse sequence developed by Schmidt-Rohr et al. [38]. The π/2 pulse to excite the ^1H spectra was 4.4 μs in all the cases. The proton magnetization was transferred to ^{13}C using a short contact time of 200 μs to avoid equilibration of the proton magnetization due to spin diffusion. The MAS rate was set to 4.5 kHz in order not to affect the proton lineshape. In our experiment, 32 increments of 3 μs were collected in the indirect ^1H dimension.

2.3. Electron paramagnetic resonance (EPR)

EPR measurements of the Cu(II)-complexes were performed at X-band on a Bruker EMX Plus Spectrometer at 20 °C. The spectrometer settings were: a microwave frequency of 9.87 GHz, a modulation field of 100 kHz, modulation amplitude of 4 G, microwave power of 0.2 mW, and 2040 points of resolution. The number of scans in all the experiments was 100.

2.4. Thermal analysis

Thermogravimetric measurements were carried out with a TA Instrument SDT Q600, under nitrogen flux over a temperature range from 20 to 400 °C with a heating rate of 10 °C min^{-1}. The average sample size was 10 mg.

3. Results

3.1. Adsorption of copper(II) ion onto the polymer materials

The adsorption data for copper ion were analyzed according to the Langmuir model, and the results are summarized in Table 1. The results were compared with other materials commonly used for the removal of copper ion and with related materials containing imidazole, triazole or pyrazole. All the materials presented high capacities for the uptake of copper ions, except polymer A. The presence of the azole unit produced a significant increase in the coordination of the metal ion. The high values of q_m and K_L obtained for the different Cu^{2+} uptake profiles were promising, considering the few reports on polymer materials bearing azole unit for the removal of metal ion from different media [39–42]. Polymer B presented higher q_m than the different materials synthesized from vinylimidazole (Table 1) [41,42]. In contrast, polymer E presented a lower q_m than *poly*(glycidylmethacrylate-*co*-pyrazole) [40]. Polymers B, C, D and E were optimal for the removal of copper ion, and, in some cases, even better than chitosan or modified chitosan [39]. Among them, polymer C had the lowest affinity constant (K_L), indicating that the presence of an azole ligand was not only involved in the ability of copper ion uptake but also probably associated with the distribution of the ligands along the polymer

Table 1
Experimental Langmuir isotherm parameters of copper ion adsorption.

Material	Langmuir isotherm	
	q_m (mg g^{-1})	K_L (L mg^{-1})
Poly(EGDE-MAA) = A	1	–
Poly(EGDE-MAA-IM) = B	67	3.7
Poly(EGDE-2MI) = C	71	0.9
Poly(EGDE-MAA-TRZ) = D	60	2.1
Poly(EGDE-MAA-PYR) = E	38	2.3
Chitosan [39]	33	2.4
Chitosan modified with EGDE [39]	46	2.3×10^{-3}
Poly(glycidylmethacrylate-*co*-imidazole) [40]	25	–
Poly(glycidylmethacrylate-*co*-triazole) [40]	18	–
Poly(glycidylmethacrylate-*co*-pyrazole) [40]	72	–
Poly(vinylimidazole)-SiO_2 [41]	45	–
Poly(vinylimidazole-*co*-acrylic acid) [42]	31	–

structure, the density of functional ligands and the flexibility of the polymer. Polymer C is a polyelectrolyte system with a single kind of ligands (imidazole ring) to coordinate the copper ions, however, the other polyampholyte systems (Polymers B, D and E) have two kind of ligands, the azole and the carboxylate groups, doing the K_L higher than in polymer C.

3.2. ^{13}C CP-MAS spectra

In order to evaluate the coordination role of the carboxylic acid in comparison with the different azole rings (triazole and pyrazole) in the Cu(II)-complexes of the polymers *poly*(EGDE-MAA-TRZ) = D and *poly*(EGDE-MAA-PYR) = E, we observed the changes in the intensity of C(1) in the ^{13}C CP-MAS spectra. The results are shown in Figs. 1 and 2. Special care was taken in the selection of the contact times during cross polarization experiment, since the relaxation times in the rotating frame were dramatically decreased as the copper ion adsorption increased (see Section 3.4). Long contact times may lead to the disappearance of some NMR signals.

For the D materials, the C(1) resonance signal disappeared when the copper ion adsorbed was approximately 23 mg of Cu(II) per gram of polymer (Fig. 1, D_{23}), whereas for the E materials, the C(1) resonance signal disappeared with 5 mg of Cu(II) per gram of polymer (Fig. 2, E_5). This indicates that the carboxylate group in this material was more significant in the uptake of Cu^{2+} than the other materials under study at low concentration of the paramagnetic ion. Note that the ^{13}C CP-MAS spectra were obtained in the same experimental conditions and with the same contact time (1.5 ms).

Fig. 3 displays the ^{13}C CP-MAS spectra of *poly*(EGDE-2MI) = C and its copper complex C_{60}. Different contact times were used to study the magnitude of the changes in signal intensity in a system that contains only imidazole groups. In this material, the amount of available ligands was around 85%, whereas the remaining 15% was N_1,N_3-disubstituted. Changing the contact time from 600 to 1000 μs in the ^{13}C CP-MAS experiment, the intensity of the signals at 122.0 and 144.8 ppm in the ^{13}C spectrum of C_{60} were highly affected (Fig. 3 and Electronic Supplementary Material, Fig. S4). This indicates that the copper ion produced a strong decrease in the relaxation times of the entire polymer, especially for the carbons nearby to the imidazole units (Fig. 3).

Other authors studying the coordination of Cu^{2+} in imidazole-containing polymers through ^{13}C CP-MAS spectra found that the disappearance or the decrease in the intensity of the signal from the imidazole ligands was associated with the metal binding to Cu^{2+}. Nevertheless, they provided no information regarding the contact time used for the ^{13}C CP-MAS spectra or the number of ligands involved in the process [43,44].

Having into account the difference in the nature of the carbons and their $T^H_{1\rho}$, we observed that in the Cu(II)-complexes of B, the imidazole carbon signals were affected by the copper ion but not at the same extent as the carboxylic acid (Fig. 4). In B_{63}, the contact time used to obtain the best signal-to-noise ratio for all the signals was 800 μs (Fig. 4c). In contrast, with a contact time of 1.5 ms, the signals of the imidazole ring had lower intensity than the C(2) corresponding to the ester carbons (Electronic Supplementary Material, Fig. S5). Nevertheless, the imidazole carbon signals were not very reliable to test the uptake of copper ions, although we know that this group participates in the coordination process because the monomeric composition of carboxylic acid ligands in polymer A was higher than in polymer B (0.65 versus 0.35) [36].

In addition, to explore changes in the coordination sphere, we performed some modifications in B and B_{63}. First, when the Cu(II)-complex B_{63} was treated with a 50 mM hydrogen peroxide solution (B^{T1}_{63}), some significant changes were observed in the ^{13}C CP-MAS spectra, as a result of the reduction of Cu(II) to Cu(I) (Fig. 4d). Here the interaction between the H_2O_2 molecules with the Cu(II) centers produced hydroxyl radicals and oxygen, with the concomitant reduction of the paramagnetic center of Cu(II) to the diamagnetic center of Cu(I), remaining 5% of Cu(II) [45]. Thus, the signal-to-noise ratio was improved as the Cu(II) centers were converted to Cu(I). Interestingly, the C(1) signal arose as a weak shoulder of the C(2) signal, indicating that the carboxylic acid group was not strongly affected by the metal ion.

In the second modification, B^{T2}_{63} presented a ^{13}C CP-MAS spectrum similar to that of the B^{T1}_{63} as well as a weak C(1) signal (Fig. 4b,e). This may indicate that, in this condition, the carboxylic acid groups were not as significant in the uptake of copper ions as in B_{63} without treatment.

Note that, in general, the ^{13}C CP-MAS spectra do not show any significant shift in the signals of the Cu(II)-complexes with respect to those in the spectra of the pure polymers.

3.3. EPR studies

Figs. S1–S4 (in supplementary information) show the X-band EPR spectra for Cu(II)-polymers at different levels of adsorption of copper ion. Table 2 displays the EPR parameters for the Cu(II)-complexes of polymers A–E and some polymers of reference.

In general, the EPR signal presents a well-resolved hyperfine structures in the parallel region that corresponds to isolated mononuclear square-planar Cu(II)-complexes with a minimum distance of 10–15 Å between them [47]. The four lines in this region arise from hyperfine coupling of the electron spin ($S = 1/2$) of the copper nucleus with its nuclear spin ($I = 3/2$).

The $A_{||}$ and $g_{||}$ values were 132 G and 2.354 in A_1 and 146 G and 2.317 in C_{32}. According to Peisach-Blumberg plots [48], these values were in the range expected for four oxygen ligands in the equatorial plane in A_1 (4O) and, for two or three nitrogen and one or two oxygen ligands in C_{32} (2N,2O/3N,1O). The oxygen ligands in C_{32} may arise from the EGDE segments (Fig. 3), which can participate in the coordination together with the imidazole moieties. Thus, in C_{32}, the expected EPR values differed from the results obtained by Annenkov et al. in Cu(II)-*poly*(1-vinylimidazole) [46], which may explain the lower value of the K_L constant of polymer C (Table 1) as compared with that of polymers B, D and E. Note that the $A_{||}$ values did not vary and the $g_{||}$ values slightly increased with the

Table 2
EPR parameters for the Cu(II)-complexes of polymers A–E, and some Cu(II)-polymers of reference.

Material	$A_{\|}$ (G)	$g_{\|}$	$g_{\perp}$	Ligating atoms
A_1	132	2.354	2.076	4O
Cu(II)-*poly*(acrylic acid) [46]	141	2.340	2.035	4O
B_8	158	2.287	2.064	3N,1O/4N
B_{26}	160	2.289	2.073	3N,1O/4N
B_{48}	152	2.294	2.075	2N,2O
B_{63}	148	2.331	2.083	1N,3O
B^{T1}_{63} (H_2O_2)	158	2.300	2.069	3N,1O/4N
B^{T2}_{63} (NaOH)	160	2.299	2.075	3N,1O/4N
Cu(II)-*poly*(1-vinylimidazole) [46]	161	2.271	2.025	4N
C_{10}	146	2.303	2.075	3N,1O/2N,2O
C_{21}	146	2.316	2.078	3N,1O/2N,2O
C_{32}	146	2.317	2.074	3N,1O/2N,2O
D_5	152	2.308	2.066	3N,1O/2N,2O
D_{10}	152	2.312	2.069	3N,1O/2N,2O
D_{23}	152	2.314	2.069	3N,1O/2N,2O
D_{40}	148	2.328	2.073	2N,2O/1N,3O
D_{50}	148	2.340	2.078	1N,3O
E_5	144	2.321	2.065	2N,2O/1N,3O
E_{12}	148	2.325	2.069	2N,2O
E_{19}	155	2.320	2.069	3N,1O/2N,2O

concentration of Cu(II) in the complexes C_{6-32}, suggesting that the surroundings of the paramagnetic ions were similar.

Interestingly, the $A_{||}$ and $g_{||}$ values differed in Cu(II)-complexes of B, D and E, ascribable to changes in the ligand environment around the sphere of the copper ion, depending on the groups available on each polymer matrix. It is important to mention that in the cases where Cu^{2+} is ligated to both nitrogen and oxygen, the assignment of structure on the basis of EPR results is not a clear-cut [48]. Thus, our EPR results were discussed in complement with ssNMR results.

In the case of Cu(II)-complexes of B and D, the EPR parameters showed that oxygen became more active in the uptake of copper ions, according with the decrease of the $A_{||}$ values and with the increase in the $g_{||}$ values with the copper concentration (see Table 2). At low concentrations of copper ion adsorbed, in B_8 or D_5, the EPR parameters ($g_{||}$ and $A_{||}$ values) indicated that the ligands might be 3N,1O/4N or 3N,1O/2N,2O respectively, according with the Peisach-Blumberg plots. Therefore, the azole ligands in B_{48} and D_{23} may be still coordinating copper, but some structural rearrangements, from B_8 to B_{48} and from D_5 to D_{23}, facilitated the participation of both carboxylic acid and imidazole moieties in the uptake of copper ion. This fact produced an increasing the adsorbed amount of metal ion due to the different coordination modes available. For that reason, the NMR carbon signal of the carboxylic acid was undetected in the ^{13}C CP-MAS spectra of B_{48} and D_{23}. Furthermore, the higher concentrations of copper ion in B_{63} and D_{50} might overlap the initial coordination modes observed in the EPR spectra of $B_{8\text{-}48}$ and $D_{5\text{-}40}$ Electronic Supplementary Material, Figs. S2 y S5.

On the other hand, while in C the same ligands were available for the coordination of the copper ion with the increasing concentration, the variation of the EPR parameters in B and D, gives evidence of different groups participating in the uptake of Cu(II).

In the case of copper complexes of polymer E, the $A_{||}$ values increased and $g_{||}$ values remain constant with the concentration of copper ion adsorbed. These results indicate that the coordination of copper ions occurred through the carboxylic acid at any concentration of Cu^{2+} ions. For E_5, the ligands could be 1N,3O and/or 2N,2O according with the Peisach-Blumberg plots, and for E_{19} the sphere of coordination was 3N,1O and/or 2N,2O, in concordance with the $g_{||}$ and $A_{||}$ values found for D_5.

It is interesting to note that the EPR spectra present some distortions in the Cu(II)-complexes C_{60} and E_{33}, as a consequence of the Cu–Cu dipolar interaction or exchange coupling.

In the case of B_{63}^{T1}, a completely different EPR spectrum was observed, as a result of the reduction of Cu(II) to Cu(I) (Fig. 5). Here, the EPR signal displayed a lower intensity than in B_{63}, because residual Cu(II) centers were observed after the action of the hydrogen peroxide solution. On the other hand, the EPR parameters were similar to those obtained in B_8. It is important to mention that the EPR spectra obtained may be the result of the overlapping of different Cu(II) environments, but in all the cases, we analyzed the highest contribution. For that reason, even when different coordination modes may coexist in B_{63}, the smaller contributions can only be inferred via the treatment with H_2O_2 in B_{63}^{T1}, where the most significant contribution observed in B_{63} (1N,3O) vanished. This treatment allowed recovering the initial situation found in B_8 (Table 2 and Fig. 5).

In the case of complex B_{63}^{T2} (Fig. 5), the increase in the $A_{||}$ and the decrease in the $g_{||}$ values observed resulted in parameters similar to those obtained for Cu(II)-*poly*(1-vinylimidazole) [46]. Here, the treatment with NaOH solution in polymer B produced the release of the proton from the imidazolium groups (protonated imidazole: R–N^+H), increasing the number of free nitrogen ligands available for copper ion uptake, leading to the same coordination mode as in Cu(II)-*poly*(vinylimidazole), N_4. When polymer B was not treated with basic solution, a number of imidazolium- and imidazole-free ligands were attached to the polymer backbone (R–N). However, when the Cu^{2+} solution was mixtured with the solid material, protons were exchanged to coordinate a copper ion, producing a decrease in the pH of the contact solution (pH = 5.0), affecting other nitrogen ligands. Thus, the ability of the imidazole ligand to coordinate copper ion was slightly affected by the pH, allowing that carboxylate or oxygen of the EGDE segment to participate in the coordination sphere. In the case of D_{55} and E_{33}, the pHs of the contact solutions were 5.3 and 6.4, respectively.

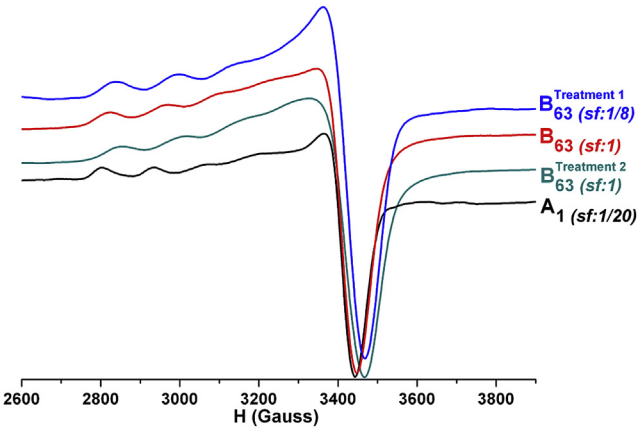

Fig. 5. EPR spectra for the copper(II) complexes A_1, B_{63}, B_{63}^{T1} and B_{63}^{T2}. (*sf*: scaling factor).

3.4. 2D ^1H-^{13}C wideline separation and relaxation time ($T_{1\rho}$) experiments

The 2D ^1H-^{13}C Wideline Separation experiments (2D WISE) showed remarkable differences among the materials bearing azole residues (Table 3 and Electronic Supplementary Material, Figs. S6 and S7). In all the cases, the full width at half height (FWHH) for

Table 3
$T_{1\rho}^C$ values (in ms) measured for the indicated polymers together with the full width at half height (FWHH) for the ^1H projection corresponding to the C(3) at 70 ppm in the 2D WISE experiments. $T_{1\rho}^C$ values were obtained by fitting the experimental data of ^{13}C magnetization vs. τ to Equation (2) or (3). The uncertainty in all FWHH values reported for the ^1H projection is less than ±2 kHz and for the $T_{1\rho}$ values the relative errors are within 5%.

Polymer	$T_{1\rho}^C$ (EGDE)[a]		$T_{1\rho}^C$ (MAA)[b]				$T_{1\rho}^C$ (HET)[c]		FWHH (kHz)
	C(3)		C(4)		C(5)		C(7)	C(8)	
C	1.9	0.6	–		–		–	3.7	57
C_{60}	1.4	0.4	–		–		–	–	51
B	2.0	0.6	0.7		–		–	3.5	59
B^{T2}	3.8	0.8	2.7	0.6	6.2	0.6	–	3.5	54
B_{63}	1.1	0.3	0.6		–		–	–	46
B_{63}^{T1}	5.5	1.0	1.5	0.4	–		–	3.7	55
B_{63}^{T2}	1.3	0.3	0.7		–		–	–	48
D	2.4	0.5	1.1		–		5.3	–	64
D_5	2.6	0.5	1.7	0.5	–		5.7	–	56
D_{10}	2.3	0.4	1.5		–		5.0	–	57
D_{23}	2.1	0.4	1.0		–		4.3	–	54
D_{40}	1.2	0.1	0.9		–		2.8	–	51
E	2.9	0.6	1.3		8.0		6.9	5.5	50
E_5	2.2	0.3	1.0		10.0		7.0	5.0	53
E_{12}	2.5	0.5	1.3		9.0		6.0	5.4	54
E_{19}	2.5	0.5	1.1		6.5		3.9	5.9	55
E_{33}	2.5	0.7	0.9		2.3		2.2	2.4	59

[a] Carbon signals of the EGDE.
[b] Methacrylic segment.
[c] Heterocyclic segment.

the ^{1}H projection corresponds to the carbon signal at 70 ppm, C(3), since it had the best signal-to-noise ratio at the 200 μs contact time used in the WISE experiments. In particular, the typical behavior of the crosslinking effect produced by the coordination of the copper ion can be seen in polymer E. In this material, the absence of disubstituted pyrazole groups and the reduction in the macromolecular mobility leads to higher FWHH values, as the concentration of coordinated Cu(II) increased (Table 3).

However, in polymer D which has a 37% of N_1,N_3-disubstitution of the triazole groups, the FWHH values decreased from 64 to 51 kHz from D to D_{40} materials. This might indicate that the macromolecular mobility was enhanced by the influence of the copper ion after the coordination process took place. The presence of the copper ion induced a rearrangement of the polymeric segments, where the carboxylic acid groups might be near the azole groups prior to the uptake of the metal ion, producing an expansion of the entire network. The net results were a balance between the reduction in the polymeric mobility, induced by the crosslinking of the copper ion, and a polyelectrolyte effect associated with the increase in the positive domains in the case of triazole. In this aspect, the polyelectrolyte effect was the main factor for the rearrangement of the different polymeric segments, producing more mobile network after the inclusion of the copper ion. The same effect was observed in B, where the FWHH values were 59 kHz (without copper ion) and 46 kHz (with copper ion, B_{63}) or 48 kHz (B_{63}^{T2}) (Table 3), indicating that the disubstitution of the imidazole ring affected the macromolecular mobility. The SEM images of B and B_{63} (Fig. 6) show that the network expansion occurred with the coordination of copper ions, associated with the polyelectrolyte effect.

Then, B_{63}^{T1} presented an increase in the FWHH values in comparison with B_{63} (Table 3). This result may indicate that the reduction from Cu^{2+} to Cu^{1+} decreased the polyelectrolyte effect, slightly reinforcing the interactions in the polymer matrix.

Additionally, ^{1}H and ^{13}C relaxation times in the rotating frame ($T_{1\rho}^{H}$ and $T_{1\rho}^{C}$) were determined for both the polymers loaded and unloaded with copper ion. The time evolution of the carbon magnetization data in both experiments was fitted to Equation (2) or (3):

$$M_C(\tau) = M_0 \times e^{-\frac{\tau}{\tau_1}} \quad (2)$$

$$\frac{M_C}{M_0}(\tau) = A \times e^{-\frac{\tau}{\tau_1}} + (1-A) \times e^{-\frac{\tau}{\tau_2}} \quad (3)$$

All the $T_{1\rho}^{H}$ and $T_{1\rho}^{C}$ values decrease with copper concentration for all the materials. Interestingly, the $T_{1\rho}^{C}$ values were specifically affected by the uptake of copper ion in the case of the signals of the C(7) and C(8) carbons, in the different materials, even when a slightly decreasing effect was observed for the other signals (Table 3 and Fig. 7). This indicates that the azole groups played a significant role in the uptake of copper ion. However, the paramagnetic effect was not observed in the MAA segment, C(4) and C(5), since these carbons were not as close to the sphere of coordination as those of the azole groups.

Particularly for C(3), the magnetization for all the samples decreased, showing a two-exponential behavior and evidencing the non-homogenous character of the materials, where the shorter $T_{1\rho}$ values corresponds to the more mobile regions.

The $T_{1\rho}^{H}$ values were more affected by the copper ions in polymer D, since the dynamics changed to a more mobile matrix than in E, where the $T_{1\rho}^{H}$ values were not decreased in the same magnitude (Fig. 7). For polymer E, although copper ions induced a reticulation of the polymer matrix, the relaxation behavior of the paramagnetic ions was the dominant effect. In addition, all the Cu(II)-complexes reached the same $T_{1\rho}^{H}$ values at their highest concentration of Cu^{2+} (Fig. 7 and Electronic Supplementary Material, Table S1).

In the case of B_{63}^{T1}, it was possible to measure the $T_{1\rho}^{C}$ value for C(8) (Table 3), since the diamagnetic effect of Cu(I) did not affect the relaxation of the ^{13}C nucleus, in contrast to that observed with B_{63} and B_{63}^{T2}.

3.5. Thermal analysis

Fig. 8 shows the thermogravimetric profiles carried out for B, C, D, E and their copper complexes. In general, a lower thermal stability was observed for all the Cu(II) complexes, as a result of the weakening in the chemical bonds after the coordination of the metal ion that produced changes in the electron density.

Matrix A showed two peaks of decomposition between 260 and 400 °C. In contrast, matrix B showed a single peak of decomposition at 390 °C, indicating that the presence of imidazole gave greater thermal stability to the polymer lattice [34]. On the other hand, this indicates that in the polymers where methacrylic acid (MAA) was used together with the crosslinking agent (EGDE), the weight loss is due to the water occluded in the polymer matrix (50–100 °C), as well as the water from the formation of anhydride groups between the carboxylic acid, at about 260 °C. Polymer C showed a thermal stability similar to that of polymer B, indicating that while the imidazole ring could be involved in the thermal stability by π–π stacking interaction, the crosslinking agent also played an important role. Moreover, imidazoles might be responsible for interacting with carboxylic acid by hydrogen bonding, to reduce the degree of decarboxylation or dehydration, giving rise to anhydrides in polymer B. This fact leads to a higher thermal stability in polymer B than in the other materials under study. B^{T2} presented a thermal degradation profile similar to polymer A, which only contains carboxylic acid as ligand [21]. This indicates that the interaction

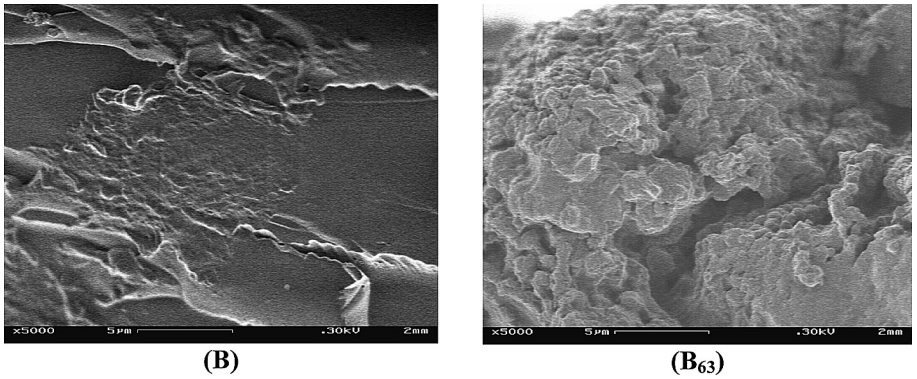

(B) **(B_{63})**

Fig. 6. SEM images of B and B_{63} materials.

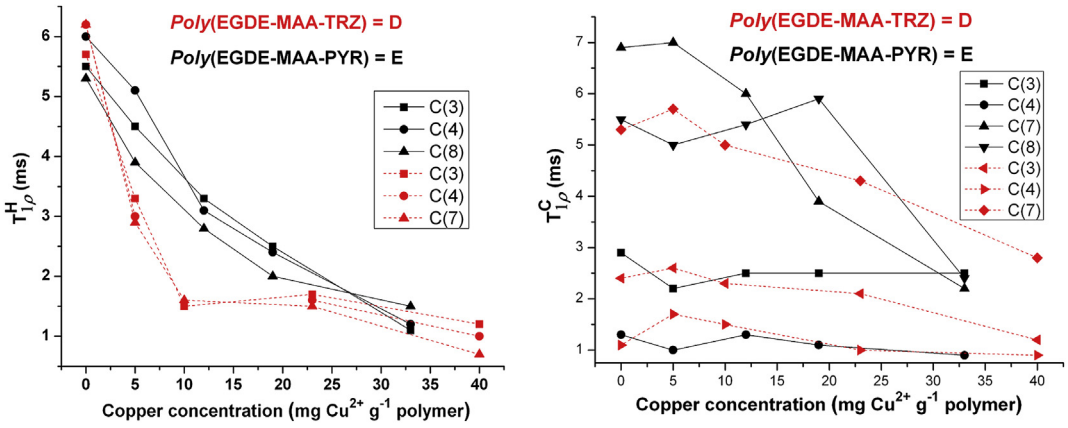

Fig. 7. Relaxation times in the rotating frame for protons and carbons ($T^H_{1\rho}$ and $T^C_{1\rho}$) for the indicated polymer and with different concentrations of adsorptive Cu^{2+}.

between imidazole and carboxylic acid groups was disturbed by the NaOH solution, and thus the carboxylic acid groups were released from the imidazole moieties, producing a higher thermal decomposition susceptibility (Fig. 8). Also, for Polymer B^{T2} the residue was around a 13%, a slightly higher than polymer B, associated with the inorganic residues of the NaOH solution used. In addition, the TG profiles of the Cu(II)-complexes of polymer B showed modifications depending on the treatment performed in the samples. For instance, the reduction from Cu^{2+} to Cu^{1+} in B^{T1}_{63} produced a reduction in the temperature of the degradation comparing to B_{63}, even when the entire network was affected by the presence of the metal ion, independently of its oxidation state.

Furthermore, the loss of mass in B^{T2}_{63} was significantly reduced in the temperature range from 200 to 300 °C in comparison with B^{T2} and B_{63}, as can be observed from the TG and DTG curves (Fig. 8). With this modification, B^{T2}_{63} presented the highest thermal stability of the B copper complexes. However, the treatment with NaOH released the acidic protons and the q_m and K_L values obtained from

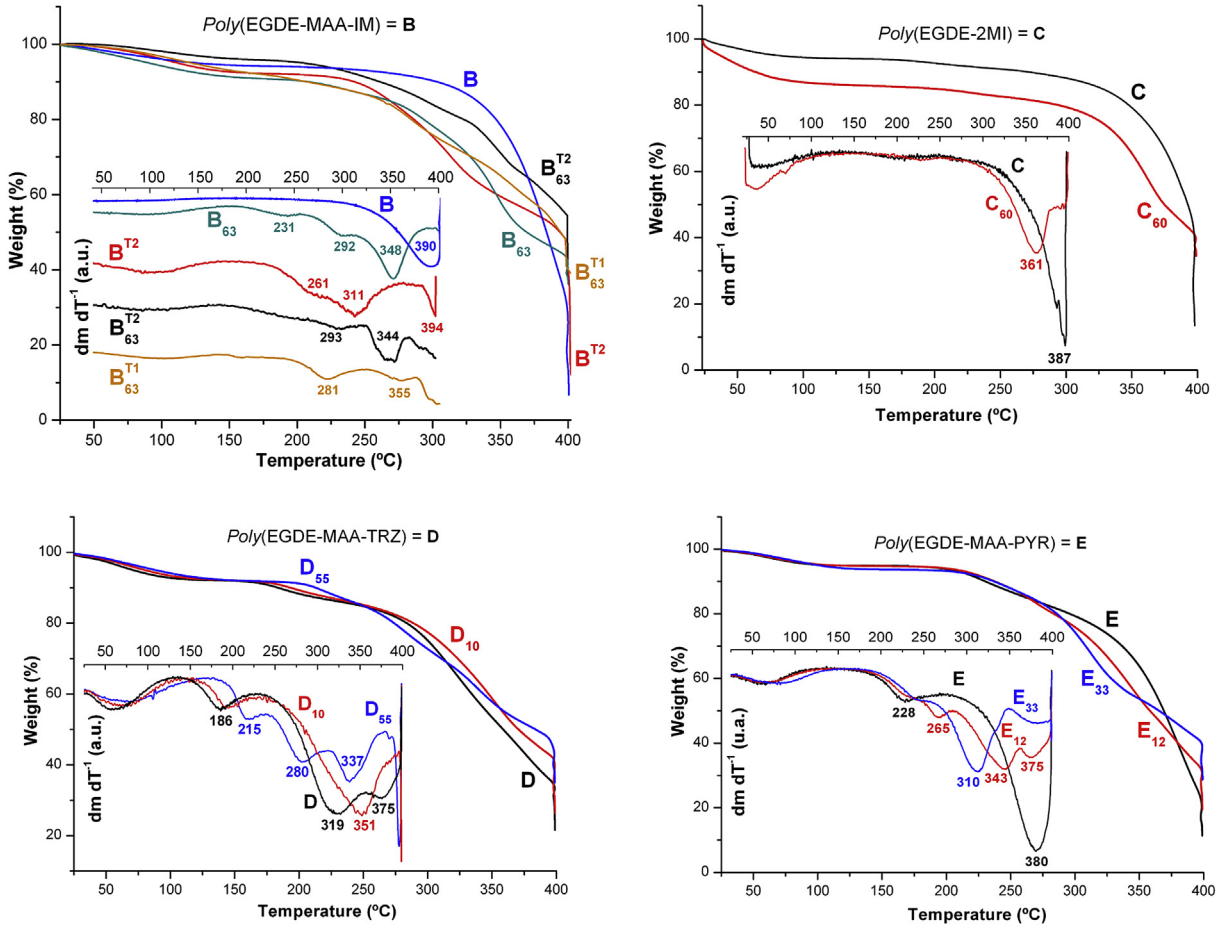

Fig. 8. TG and DTG curves for polymer B–E and their Cu(II)-complexes.

the coordination of Cu(II) ions, were practically the same. Thus, the rest of the carboxylate groups probably interact with imidazolium groups (disubstituted imidazole groups), preventing their thermal degradation.

On the other hand, materials D and E, with triazole or pyrazole respectively, had completely different profiles and even a lower thermal stability than the others. This indicates that the carboxylic acid groups might be more susceptible to degradation than in B, probably by a decreased ability to interact with the pyrazole and triazole rings or because they were away from the azole groups. Although this phenomenon is difficult to explain, the proposed hypothesis is possible since when B was treated with copper ion solutions, the carboxylic acid groups were more susceptible to break down and caused a DTG profile similar to that in A, D, E and their Cu(II)-complexes (Fig. 8). In turn, while the ions of Cu(II) were responsible for a lower thermal stability in the complexes obtained from B, matrix C with 67 mg of coordinated Cu(II) per gram of polymer experienced only a shift of 30 °C at peak degradation. This may explain why the thermal susceptibility in matrices B, D and E changed with the content of Cu(II) because different functional groups were involved in the uptake of copper ion, in agreement with the results obtained in this work by ssNMR and EPR studies. Note that in all the Cu(II) complexes a residual weight was observed due to residual cupric salts after the degradation of the organic matrix. These residue were increased when the amount of Cu(II) ion coordinated was higher.

4. Conclusions

Herein, we demonstrated that ssNMR, combined with EPR, can provide a powerful approach to elucidate details of the coordinating ligands in copper-polymer complexes. In particular, the ^{13}C CP-MAS spectra were determinant because the carbon of the carboxylate ligands particularly close to the Cu^{2+} ion relaxed rapidly, thus preventing its detection. At low concentrations of $CuSO_4$ solution, the uptake of Cu^{2+} ions took place preferentially through the azole groups, with less participation of the carboxylate groups. However, in the case of imidazole and triazole, as the concentration of $CuSO_4$ increased, the azole ligands became less active in the new sites for copper ion. In the case of the polymer containing pyrazole (E), the copper ions were preferentially coordinated through the carboxylate ligands at any concentration of the metal ion. Then, the increasing values of $A_{||}$ as the concentration of copper ion adsorbed increased indicate that the nitrogen ligands were mainly involved at high concentrations of Cu^{2+} in E_{33}.

In materials B, D, and E, the presence of the azole groups in the polymer backbone produced an increase in the maximum loading capacities in comparison with polymer A, but this increase was accompanied with the carboxylate ligands according with our NMR and EPR results.

The molecular dynamics and the interactions of the different ligands in each polymer network and their Cu(II)- or Cu(I)-complexes were assessed through thermal analysis, ^{13}C CP-MAS, $T_{1\rho}$ and 2D WISE experiments.

Finally, the interaction between the carboxylic acid and imidazole moieties in polymer B led to an increase in the thermal stability as compared to the rest of the polymer matrixes studied here, as shown with B^{T2}.

Acknowledgments

We thank the financial support from CONICET (PIP 2010-12/441 and 754), Universidad de Buenos Aires (UBACyT 2010-12/109), SeCyT Universidad Nacional de Córdoba, and ANPCYT PICT 2010-1096 and 2012-0151. J.M. Lázaro Martínez thanks CONICET for his postdoctoral fellowships. The authors thank A.M. Gennaro and C. Brondino from the Universidad del Litoral (UNL, Santa Fé, Argentina) for the assistant in the EPR measurements.

Appendix A. Supplementary data

Supplementary data related to this article can be found at http://dx.doi.org/10.1016/j.polymer.2013.07.036.

References

[1] Anderson EB, Long TE. Polymer 2010;51:2447–54.
[2] Schachschal S, Balaceanu A, Melian C, Demco DE, Eckert T, Richtering W, et al. Macromolecules 2010;43:4331–9.
[3] Tsitsilianis C, Stavrouli N, Bocharova V, Angelopoulos S, Kiriy A, Katsampas I, et al. Polymer 2008;49:2996–3006.
[4] Buwalda SJ, Dijkstra PJ, Feijen J. J Polym Sci Part A: Polym Chem 2012;50:1783–91.
[5] Zhang J, Su CY. Coord Chem Rev 2013;257:1373–408.
[6] Ishiwata T, Furukawa Y, Sugikawa K, Kokado K, Sada K. J Am Chem Soc 2013;135:5427–32.
[7] Ramírez E, Burillo SG, Barrera Díaz C, Roa G, Bilyeu B. J Hazard Mater 2011;192:432–9.
[8] Kampalanonwat P, Supaphol P. Ind Eng Chem Res 2011;50:11912–21.
[9] Hadjikallis G, Hadjiyannakou SC, Vamvakaki M, Patrickios CS. Polymer 2002;43:7269–73.
[10] Noh JG, Sung YJ, Geckeler KE, Kudaibergenov SE. Polymer 2005;46:2183–90.
[11] Rivas BL, Pereira ED, Moreno Villoslada I. Prog Polym Sci 2002;28:173–208.
[12] Ravikumar L, Kalaivani SS, Murugesan A, Vidhyadevi T, Karthik G, Dinesh Kirupha S, et al. J Appl Polym Sci 2011;122:1634–42.
[13] Kinoshita T, Ishigaki Y, Nakano K, Yamaguchi K, Akita S, Nii S, et al. Sep Purif Technol 2006;49:253–7.
[14] Chujo Y, Sada K, Saegusa T. Macromolecules 1993;26:6320–3.
[15] Fiore GL, Klinkenberg JL, Fraser CL. Macromolecules 2008;41:9397–405.
[16] Fullenkamp DE, He L, Barrett DG, Burghardt WR, Messersmith PB. Macromolecules 2013;46:1167–74.
[17] Jung JH, Lee JH, Silverman JR, John G. Chem Soc Rev 2013;42:924–36.
[18] Lee H, Lee JH, Kang S, Lee JY, John G, Jung JH. Chem Commun 2011;47:2937–9.
[19] Samai S, Biradha K. Chem Mater 2012;24:1165–73.
[20] Lin CC, Metters AT. J Biomed Mater Res A 2007;83:954–64.
[21] Pfister A, Fraser CL. Biomacromolecules 2006;7:459–68.
[22] Qiu Z, He Y, Liu X, Yu S. Chem Eng Process 2005;44:1013–7.
[23] Fathima NN, Aravindhan R, Rao JR, Nair BU. Chemosphere 2008;70:1146–51.
[24] Sulakova R, Hrdina R, Soares GMB. Dyes Pigm 2007;73:19–24.
[25] Lázaro Martínez JM, Leal Denis MF, Piehl LL, Rubín de Celis E, Buldain GY, Campo Dall'Orto V. Appl Catal B 2008;82:273–83.
[26] Sergeyeva TA, Slinchenko OA, Gorbach LA, Matyushov VF, Brovko OO, Piletsky SA, et al. Anal Chim Acta 2010;659:274–9.
[27] Magdesieva TV, Dolganov AV, Yakimansky AV, Goikhman MY, Podeshvo IV, Vladislav V, et al. Electrochim Acta 2008;53:3960–72.
[28] Chen W, Boven G, Challa G. Macromolecules 1991;24:3982–7.
[29] Chen W, Challa G. Polymer 1990;31:2171–7.
[30] Kowalik Jankowska T, Ruta Dolejsz M, Wisniewska K, Lankiewicz L, Kozlowski H. J Chem Soc Dalton Trans 2000;24:4511–9.
[31] Aronoff Spencer E, Burns CS, Avdievich NI, Gerfen GJ, Peisach J, Antholine WE, et al. Biochemistry 2000;39:13760–71.
[32] Drew SC, Barnham KJ. Acc Chem Res 2011;44:1146–55.
[33] Pithadia AS, Lim MH. Curr Opin Chem Biol 2012;16:67–73.
[34] Lázaro Martínez JM, Chattah AK, Monti GA, Leal Denis MF, Buldain GY, Campo Dall'Orto V. Polymer 2008;49:5482–9.
[35] Fang X, Chen R, Xiao L, Chen Q. Polym Int 2011;60:136–40.
[36] Lázaro Martínez JM, Chattah AK, Torres Sánchez R, Buldain GY, Campo Dall'Orto V. Polymer 2012;53:1288–97.
[37] Fung BM, Khitrin AK, Ermolaev K. J Magn Reson 2000;142:97–101.
[38] Schmidt Rohr K, Clauss J, Spiess HW. Macromolecules 1992;25:3273–7.
[39] Wan Ngah WS, Endud CS, Mayanar R. React Funct Polym 2002;50:181–90.
[40] van Berkel PM, Driessen WL, Reedijk J, Sherrington DC, Zitsmanis A. React Funct Polym 1995;27:15–28.
[41] Wang R, Men J, Gao B. Clean: Soil, Air, Water 2012;40:278–84.
[42] Rivas BR, Pereira E, Jara M, Esparza C. J Appl Polym Sci 2006;99:706–11.
[43] Wu KH, Chang TC, Wang YT, Hong YS, Wu TS. Eur Polym J 2003;39:239–45.
[44] Andersson M, Hansson Ö, Öhrström L, Idström A, Nydén M. Colloid Polym Sci 2011;289:1361–72.
[45] Lázaro Martínez JM, Rodríguez Castellón E, Torres Sánchez RM, Buldain GY, Campo Dall'Orto V. J Mol Catal A: Chem 2011;339:43–51.
[46] Annenkov VV, Danilovtseva EN, Saraev VV, Mikhaleva AI. J Polym Sci Part A: Polym Chem 2003;41:2256–63.
[47] Hasty EF, Colburn TJ, Hendrickson DN. Inorg Chem 1973;12:2414–21.
[48] Peisach J, Blumberg WE. Arch Biochem Biophys 1974;165:691–708.